DOI: 10.26599/FSHW.2025.9250513

Contents lists available at SciOpen

Food Science and Human Wellness

journal homepage: https://www.sciopen.com/journal/2097-0765

China Food Publishing Co.

Total glycosides of *Cistanche deserticola* enhance the inhibitory effect of Sorafenib on mice with hepatocellular carcinoma

Duo Feng[1,2,3], Shao-shi Zhang[1,2], Shi-qi Zhou[1,2], Meng-jie Li[1,3], Xian-chun Wang[4], Yu Guo[1], Jian Zhao[1], Wen-jie Yan[1,2,*] , Jing Wang[3,*]

[1.] *College of Biochemical Engineering, Beijing Union University, Beijing 100023, China*

[2.] *Beijing Key Laboratory of Bioactive Substances and Functional Food, College of Biochemical Engineering, Beijing Union University, Beijing 100023, China*

[3.] *Institute of Food and Nutrition Development, Ministry of Agriculture and Rural Affairs, Beijing 100081, China*

[4.] *Administration for Market Regulation of Dongsheng District, Ordos, Inner Mongolia 017000, China*

ABSTRACT: Long-term use of Sorafenib (SOR) in patients with hepatocellular carcinoma will lead to drug resistance, leading to diarrhea, weight loss and other adverse reactions. *Cistanche deserticola*, as a homologous substance of medicine and food, its total glycosides (TG) have anti- hepatocellular carcinoma activity. This paper aimed to explore the anti-hepatocellular carcinoma effect of TG combined with SOR on mice and its mechanism. In this study, according to the previous research of experts, the dosage of 30mg/kg SOR was selected, aiming at giving consideration to the anti-tumor effect and reducing toxicity. Specifically, HepG2 cells were used to establish a subcutaneous tumorigenic model. Histological changes, oxidative stress, immune regulation and intestinal metabolism and microbial composition of mice were detected. It was found TG did not affect the normal growth of mice without any toxic side effects and could synergize with SOR to inhibit tumor growth. HE results found mice in TG group had more complete hepatocyte structure and less pathological changes in liver. The tumor tissue cells became rare and necrotic. TUNEL staining results revealed that TG could significantly promote apoptosis of HepG2 cells, but at a lower level than SOR. In addition, the content of CAT (Catalase), SOD (Superoxide Dismutase) and ALT/GPT (Glutamic-pyruvic transaminase) increased, AST/GOT (Aspartate aminotransferase) and AKP/ALP (Alkaline phosphatase) decreased, indicating TG could effectively reduce liver lesions. TG could also decrease the content of Interleukin-2 (IL-2), Interleukin-17 (IL-17), Tumour necrosis factor-α (TNF-α), etc., and increase interferon-γ (IFN-γ), granulocyte-macrophage colony stimulating factor (GM-CSF). Meanwhile, immunohistochemistry was used to observe the decreased expression of Ki67, β-catenin and Dishevelled (Dsh) proteins and the increased GSK-3β in the tumor tissues, it was presumed that TG exerted its anti-hepatocellular carcinoma activity through the Wnt/β-catenin signaling pathway. Most importantly, TG could synergize with SOR to regulate metabolic levels in the gut, balance intestinal microbial composition, and increase the abundance of beneficial intestinal bacteria. In conclusion, the results showed that TG (64mg/kg) could assist SOR (30mg/kg) to inhibit the development of hepatocellular carcinoma, provide some theoretical basis and technical support. *Cistanche deserticola*, as a homologous substance of medicine and food, its combination with SOR can provide a new idea for the treatment of hepatocellular carcinoma and its future application potential is worth further exploration and development.

***Corresponding author**
wangjing07@caas.cn, meyanwenjie@126.com

Received 21 April 2024
Received in revised from 10 May 2024
Accepted 6 January 2025

Keywords: *Cistanche deserticola*, anti-hepatocellular carcinoma, total glycosides, sorafenib, Wnt/β-catenin signaling pathway

1. Introduction

Liver cancer is a common malignant tumor [1]. There were over three quarters of a million liver cancer deaths worldwide in 2022, positioning liver cancer as the third leading cause of cancer death after lung and colorectum and the sixth most frequently diagnosed, with an estimated 865,000 new cases and 757,948 deaths in 2022 [2]. According to different tissue heterogeneity characteristics, they can be divided into two main types, primary and secondary. Among them, primary hepatocellular carcinoma is a common tumor with high morbidity and mortality worldwide, mainly including hepatocellular carcinoma (HCC), intrahepatic cholangiocarcinoma (ICC), and combined hepatocellular carcinoma-cholangiocarcinoma (cHCC-CC), with global incidence rates of 75%-85%, 10%-15%, and 1%-4.7%, respectively [3, 4].

Liver cancer has a low curable rate and a high mortality rate, so people should usually focus on prevention [5]. *Cistanche deserticola*, as a homologous medicine and food substance, could be used in the treatment of liver cancer to prevent the disease in the early stage and assist in the treatment of liver cancer in the middle and late stages, so as to take care of both prevention and treatment at the same time. The active components contained in *Cistanche deserticola*, for example, phenylethanol glycosides have some anti-liver cancer effects and inhibited tumor growth in H22 tumor-bearing mice by inducing tumor cell autophagy [6]. It also could reduce liver damage and improve immunity in tumor-bearing mice [7], regulated the cell cycle, induce apoptosis in HepG2 cells [8]. Sorafenib (SOR) is a muti-target tyrosine kinase inhibitor (TKI), which could promote apoptosis, reduce angiogenesis and inhibit tumor cell proliferation. At present, SOR is an effective first-line drug for advanced HCC, which can prolong the survival of patients with HCC and reduce the risk of tumor progression [9]. Nevertheless, some patients may still have adverse reactions, such as gastrointestinal reactions, skin reactions, hypertension, and are likely to produce drug resistance within 6 months [10, 11]. A study had found that compared with monotherapy, triple combination SOR-raloxifene-loratadine may be a novel promising approach in the treatment of liver cancer patients [12]. Other study had found that berberine combined with SOR is able to inhibit the proliferation of hepatocellular carcinoma cells and induce apoptosis, which provided evidence for further clinical investigation in HCC patients with SOR resistance [13]. This suggested that the combination of traditional Chinese medicine and drugs may be a promising treatment strategy [14]. Whether the total glycosides (TG) of *Cistanche deserticola* and SOR have complementary effects and reduce side effects is worth exploring to provide a more comprehensive treatment plan for patients with hepatocellular carcinoma.

Gut microbiome is considered to be one of the key elements to regulate host health [15], can affect metabolism, inflammation, immune response and disease conditions, including cancer [16]. There is a close two-way relationship between liver and intestinal microbiome (called intestinal - liver axis) [17]. Intestinal microbiome and its matabolites will affect the liver homeostasis, destroy the normal intestinal microflora balance, that is, intestinal micro-ecology imbalance, which can lead to various liver disease, while the liver

mainly affects the composition of intestinal microbiome, intestinal barrier integrity and intestinal permeability [18, 19]. Many studies have shown that HCC patients have different microbial characteristic from non-HCC group [20, 21]. In addition, some experts have suggested that targeting the gut-microbiota-liver axis could inhibit the development of HCC in mice and rats to provide potential treatment for clinical research [22-24]. Therefore, intestinal microbiome plays a key role in hepatocellular carcinoma.

A growing body of research demonstrating TG's anti-hepatocellular carcinoma properties, making it a potential anti-cancer medicine [25-27]. Not only as an independent treatment method, but also as a means to enhance the existing treatment options for advanced HCC. In this study, we evaluated whether TG enhanced the potential of SOR in the treatment of hepatocellular carcinoma in mice, and provided a scientific basis for future drug development and treatment programs.

2. Materials and methods

2.1 Materials

HepG2 cells were obtained from Cell Center of China Academy of Medical Sciences. Total Glycosides of *Cistanche deserticola* was provided by Inner Mongolia Sankou Technology Co., Ltd. (Ordos, Inner Mongolia, China) [26]. 4% paraformaldehyde, xylene (AR), and ethanol absolute (AR) were purchased form Sinopharm Chemical Reagents Co., Ltd. (Beijing, China). Sorafenib Tosylate was purchased by Shanghai Yuanye Biotechnology Co., Ltd. (Shanghai, China). The assay kits for determining SOD (A001-3-2), CAT (A007-2-1), GOT/AST (C010-2-1), GPT/ALT (C009-2-1) and ALP/AKP (A059-2-2) levels were provided by Nanjing Jiancheng Bioengineering Institute (Nanjing, China). TUNEL kit (C1089) was purchased from Beyotime Biotechnology (Shanghai, China). Primary antibodies against β- Catenin and Ki67 were purchased from ABclonal (Cambridge, Boston, USA) and abcam Biotechnology Co., Ltd. (Cambridge, UK) separately. Primary antibodies against GSK3β and Dsh were purchased from Bioss Biotechnology Co., Ltd. (Beijing, China).

2.2 Cell culture and subcutaneous tumorigenesis

HepG2 hepatocellular carcinoma cells were grown to 90% of the culture flask for passaging, after passaging for 3 times, trypsin digestion was used, and complete culture solution was used to terminate the digestion of the cells, which were collected and counted. The cells were resuspended in PBS to 2×10^7 cells/mL, and then 0.1 mL of the cell suspension was inoculated subcutaneously with a 1 mL disposable syringe at the right hind leg of the mouse, and the tumor nodules could be palpated 5 d after inoculation.

2.3 Animals and experimental design

Male Balb/c-nu mice (4~6 weeks old) were purchased by Beijing Huafukang Biotechnology Co., Ltd (Beijing, China). The animal experimental protocol was authorized by the Animal Care and Use Ethics Committee of Beijing Union University (Approval No: 20200914), and all experiments were conducted in accordance with the Guide for the Care and Use of Laboratory Animals. All mice were housed in specific

pathogen free (SPF) animal facilities, at a 12-hour light/dark cycle, a temperature of (26 ± 1)℃ and a humidity of (60 ± 5)%. They were fed adaptively for 1 week before the experiment.

After mice were inoculated with HepG2 hepatocellular carcinoma cells for 7 d, animals with successful modelling were randomly divided into 4 groups. They were the model (Mol) group (saline, n=6), the TG-treated group (TG with the final concentration of 64mg/kg after being dissolved in water, n=6), the sorafenib-treated group (SOR with final concentration 30 mg/kg [28, 29] after being dissolved in water, n=7), and the combination group (64 mg/kg TG and 30 mg/kg SOR dissolved in water, n=6). The dosage was administered at 10 mL/kg by gavage for 18 d. The mice were weighed every 2-3 d, and the tumor volume was measured every 4-5 d. They were weighed after the final dose, blood was taken from the eyeballs, and were decapitated and executed. Then dissected and stripped of heart, liver, spleen and tumor tissues. Finally, the individual tissues were weighed and the organ index was calculated, and the dissected tumor tissues were weighed and the tumor inhibition rate was calculated.

$$Tumor\ \ inhibition\ \ rate(\%) = \frac{Average\ \ tumor\ \ volume\ \ of\ \ model\ \ control\ \ group - Average\ \ tumor\ \ volume\ \ of\ \ treated\ \ group}{Average\ \ tumor\ \ volume\ \ of\ \ model\ \ control\ \ group} \times 100\%$$

$$Organ\ \ index(\%) = \frac{Organ\ \ weight}{Body\ \ weight} \times 100\%$$

2.4 Hematoxylin-eosin (HE) staining for histopathological changes

Firstly, the liver and tumor tissues were fixed using 4% paraformaldehyde and then paraffin-embedded, and cut into 4 μm slices. And they were stained with hematoxylin-eosin (HE) staining, and finally the pathological changes of each tissue were observed under an optical microscope at 200X magnification and photographed for analysis.

2.5 TUNEL assay for tumor tissue

The tumor tissue was dewaxed in xylene, 20 μg/mL DNase-free proteinase K was added dropwise, and proteinase K was washed with PBS. Prepared the appropriate TUNEL solution and mix well. Following washing, 50 μL of TUNEL solution was added to the samples and incubated for 60 min at 37℃ in the dark. The slices were taken out, washed and sealed using an anti-fluorescence quenching solution. Observed under fluorescence microscope (excitation wavelength 550 nm, emission wavelength 570 nm).

2.6 Detection of antioxidant indexes in liver tissue and liver function tests

Liver tissue was accurately weighed with 9 times the volume of saline. It was sheared and ultrasound homogenized in an ice water bath. Centrifuged the suspension, then took the supernatant and put it into 4℃ to be tested. The protein concentration of each sample was measured using the bicinchoninic acid assay (BCA) and the liver SOD, CAT, GOT, GPT, AKP contents were measured according to the corresponding kits.

2.7 Serum immune factors assay

Blood was taken from the eyeballs of mice, and the whole blood was coagulated at room temperature for 30 min, then centrifuged at 2500 g for 10 min to collect serum. The serum was diluted with the assay buffer

provided in the kit at a ratio of 1:2 before testing. Allow all reagents to warm to room temperature (20-25℃) before use in the assay. Added 200 μL wash buffer per well in 96-well plate and shook 10 min. Followed the immunoassay procedure according to the MILLIPLEX® panel and kit contents. Finally, run plate on Luminex® 200™, HTS, FLEXMAP 3D®, MAGPIX® instrument with xPONENT® software or xMAP® INTELLIFLEX instrument with INTELLIFLEX software. Lately, the Median Fluorescent Intensity (MFI) data was analyzed using a 5-parameter logistic method for calculating cytokine concentrations in samples.

2.8 Immunohistochemistry

Immunohistochemical detection of Ki67, β-catenin, Dsh, GSK-3β of tumor tissues. Firstly, the tumor tissues were prepared into paraffin sections using paraformaldehyde fixation, antigen repair, and immune reaction in sequence. Finally, the immunohistopathological changes of the tumor were observed under optical microscope. Image pro plus was used to analyze the figures and the average optical density values were used to represent the antibody positive expression rate.

2.9 Sequencing of intestinal contents

Mouse intestinal contents were collected in cryopreservation tubes for experiment analysis. 16S Sequencing of 16S rDNA amplicon was conducted by Applied Protein Technology Co., Ltd. (Shanghai, China). First, total genome DNA from samples was extracted using CTAB/SDS method and assayed for purity and concentration. Then 16S V3-V4 genes were amplified used the specific primer with the barcode. Polymerase Chain Reaction (PCR) products was mixed in equidensity ratios and was purified with AxyPrepDNA Gel Extraction Kit (AXYGEN, San Francisco, USA). Finally, sequencing libraries were generated using NEB Next®Ultra™DNA Library Prep Kit for Illumina (NEB, USA). The library was sequenced on an Illumina Miseq/HiSeq2500 platform and 250bp/300bp paired-end reads.

2.10 Untargeted metabolomics of intestinal contents

We collected mouse intestinal contents for experiments. Samples were extracted using pre-cooled methanol/acetonitrile/water solution (2:2:1), vortexed to mix thoroughly, and centrifuged at 14,000 g for 20 min at 4℃, and the supernatant was taken. Analysis was performed using an UHPLC (1290 Infinity LC, Agilent Technologies, Santa Clara, CA, USA) coupled to a quadrupole time-of-flight (AB Sciex TripleTOF 6600, Framingham, MA, USA) to collect the first and second spectrograms in Shanghai Applied Protein Technology Co., Ltd. Finally, XCMS software was used to determine compound identification and to analyze differences between metabolites (Applied Protein Technology Co., Ltd.) [30, 31].

2.11 Statistical analysis

One-way Analysis of Variance (ANONA) was utilized to determine statistically significant differences and process data graphics by using SPSS 25.0 statistical software and Graphpad prism 8.0.2, separately. Shapiro test function was used to judge whether the data conformed to the normal distribution. If the data conformed to to normal distribution, aov function was used to preform ANONA and drawed TukeyHSD to analyze the actual differences between groups to get P value. When it did not conform, Kurskal-Wallis was

used to get the P value. All results are presented as mean ± SD. Different letters indicate significant differences between groups at the $P < 0.05$ level.

3. Results and disscusions

3.1 Signs in mice with hepatocellular carcinoma

Our team previous studies found that TG significantly inhibited HepG2 cell proliferation and tumor volume growth, induced apoptosis, facilitated cell necrosis at both *in vitro* and *in vivo* levels [25, 27, 32]. To determine whether the feeding intervention processes would affect the normal growth of the mice, we followed the growth, diet, and mobility of the mice during the feeding period. It was found from Table 1 and Figure 1 that the mice had normal body weight growth and normal diet during the whole feeding process. With the continuous growth of the tumor, at the late stage of the intervention, the mice in the Mol group had poor mental status, slow movement, decreased appetite and blanched skin. The mice in the other treatment groups had good mental status, rosy skin and normal activity. Interestingly, there was no significant difference in body weight (BW) between groups of mice ($P < 0.05$). The volume and growth rate of tumor will have an impact on body weight. If the tumor is small or grows slowly, the consumption of nutrients in the host may be relatively low, so the weight difference may not be obvious.

Table 1 Effect of TG on body weight of mice with hepatocellular carcinoma

Body weight(g)	Mol	TG	SOR	TG-SOR
Day 0	25.37 ± 0.85	24.47 ± 1.60	24.98 ± 1.02	24.93 ± 0.67
Day 3	25.50 ± 0.91	25.27 ± 1.52	25.10 ± 1.36	25.00 ± 0.55
Day 6	26.03 ± 1.24	25.67 ± 1.54	25.58 ± 1.32	25.58 ± 0.82
Day 10	26.42 ± 1.27	25.75 ± 1.57	25.83 ± 1.07	25.67 ± 1.03
Day 13	26.67 ± 1.49	25.97 ± 1.71	26.17 ± 1.41	25.88 ± 1.10
Day 18	27.40 ± 1.60	27.15 ± 1.36	26.83 ± 1.44	26.50 ± 1.00

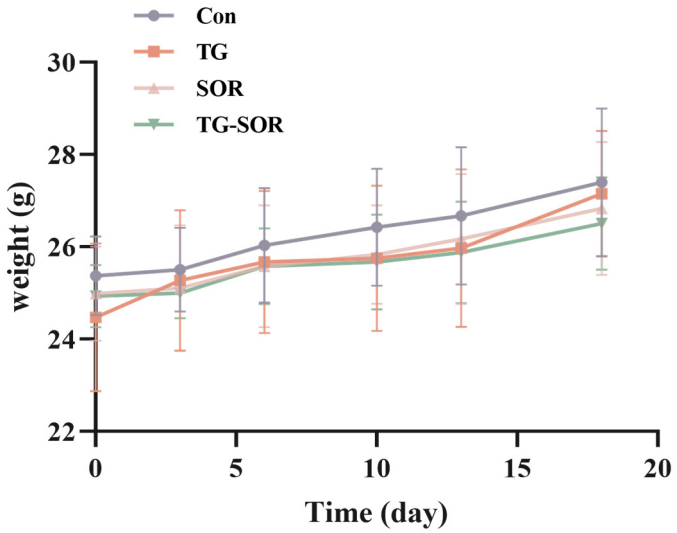

Figure 1 Effect of TG on body weight of mice with hepatocellular carcinoma

As shown in Table 2, compared with the Mol group, the liver index of the TG-treated mice decreased ($P < 0.05$), while the liver index of the SOR group increased ($P > 0.05$). The spleen index of treatment groups was higher than Mol group, TG-SOR group was the highest, and there was no significant difference among the

groups. As can be seen in Table 2, compared with Mol group, the tumor weight of each group was lower, indicating that TG had a certain degree of inhibition on the tumors of mice with hepatocellular carcinoma *in vivo*. Among them, TG-SOR had the largest tumor inhibition rate of 20.66%. Due to the individual differences of mice and the difference of organism immunity, there was no significant difference in the tumor inhibition rate between the groups ($P > 0.05$). We ensured that the inoculation number of cells, feeding management, and gastric perfusion methods were consistent, but the sensitivity of individual mice to tumor cells may also be influenced by other factors such as immune state, activation of inflammatory bodies, and tumor micro-environment. In the future, we need expand the number of mice for in-depth study, reduce the errors in the experiment process and ensure the accuracy and reliability of the data.

Table 2 Organ indexes and tumor inhibition rates of mice with hepatocellular carcinoma

groups	Liver index（%）	Spleen index（%）	Tumor weight（g）	tumor inhibition rates（%）
Mol	5.94 ± 0.49^{a}	0.43 ± 0.10	0.55 ± 0.73	-
TG	4.88 ± 0.43^{ab}	0.48 ± 0.15	0.54 ± 0.38	0.60
SOR	5.98 ± 0.52^{a}	0.49 ± 0.15	0.46 ± 0.24	16.27
TG-SOR	5.81 ± 0.23^{a}	0.57 ± 0.22	0.43 ± 0.29	20.66

Different letters indicate significant differences between groups at the $P < 0.05$ level.

We could find by Table 3 that, compared with Mol group, when the cancer cells rapidly proliferate and the tumor volume was constantly growing, the treatment had a certain effect of inhibiting the tumor volume *in vivo*. And the end of administration, we could also obviously observe that the tumor volume of the treatment group was smaller than Mol group. Moreover, tumor volume of TG-SOR group was in slow growth in the early stage, with the smallest growth rate. It indicated that TG can be used as nutritional intake to play a role in assisting targeted SOR treatment of hepatocellular carcinoma in the early stage and as a traditional Chinese medicine treatment to inhibit the tumor growth in the late stage.

Table 3 Tumor volume in mice with hepatocellular carcinoma

Tumor volume (mm^3)	Number of measurements (times)			
	1	2	3	4
Mol	49.29 ± 33.59	196.24 ± 181.03	575.54 ± 586.93	860.25 ± 925.66
TG	35.60 ± 40.95	220.79 ± 142.72	411.70 ± 147.38	696.98 ± 379.80
SOR	69.81 ± 31.11	163.47 ± 56.71	518.00 ± 248.91	796.40 ± 424.17
TG-SOR	71.33 ± 37.33	133.96 ± 106.06	327.29 ± 265.41	620.85 ± 484.67

3.2 The liver and tumor tissues of mice with hepatocellular carcinoma

In HE staining, hematoxylin stain is alkaline and causes the nuclei of the cells to take on a bluish-purple color. Eosin stain is acidic and causes the cytoplasm and extracellular matrix to stain in color red. As shown in Figure 2A, HE analysis of liver tissue from mice, the Mol group showed irregular structure and particulate cellular cytoplasm, most hepatocytes were swollen in size, cytoplasmic sparseness, enlarged cellular spaces, and some of the hepatocytes showed peripheral microscopic dysplasia cell infiltration phenomena[7]. The structure of hepatocytes in the livers of mice in each treatment group was more regular and necrosis was reduced. In addition, the hepatocytes were polygonal or round-like with light eosinophilic staining, the nuclei

were round or polygonal and centrally located, the chromatin was sparse and the nuclear membranes were clear. Among them, the pathological changes were the mildest in the TG-SOR group. The results of HE staining of tumor tissues (Figure 2B) showed that the tumor cells of the mice in the Mol group showed diffuse growth, with dense and disordered irregular arrangement, and no tissue structure was seen. The cancer cells were richer in cytoplasm, the nuclei were large and overlapped with each other, and typical pathological nuclear division was seen. The distribution of tumor cells in each treatment group became more and more sparse, the nuclei were small in size, the degree of vacuolar degeneration increased, the cytoplasm was pale, the cells were ruptured or even lysed and necrotic phenomenon, and the structure was unclear. Of these, the tumor cell necrosis effect was most obvious in the TG-SOR group, followed by SOR. These results demonstrated that TG could not only improve the ability of protect liver [33], but also could help SOR to destroy the structure of tumor cells and cause cell necrosis in tumor tissues. They intuitively reflected the hepatoprotective and anti-cancer effects of *Cistanche* in mice with hepatocellular carcinoma.

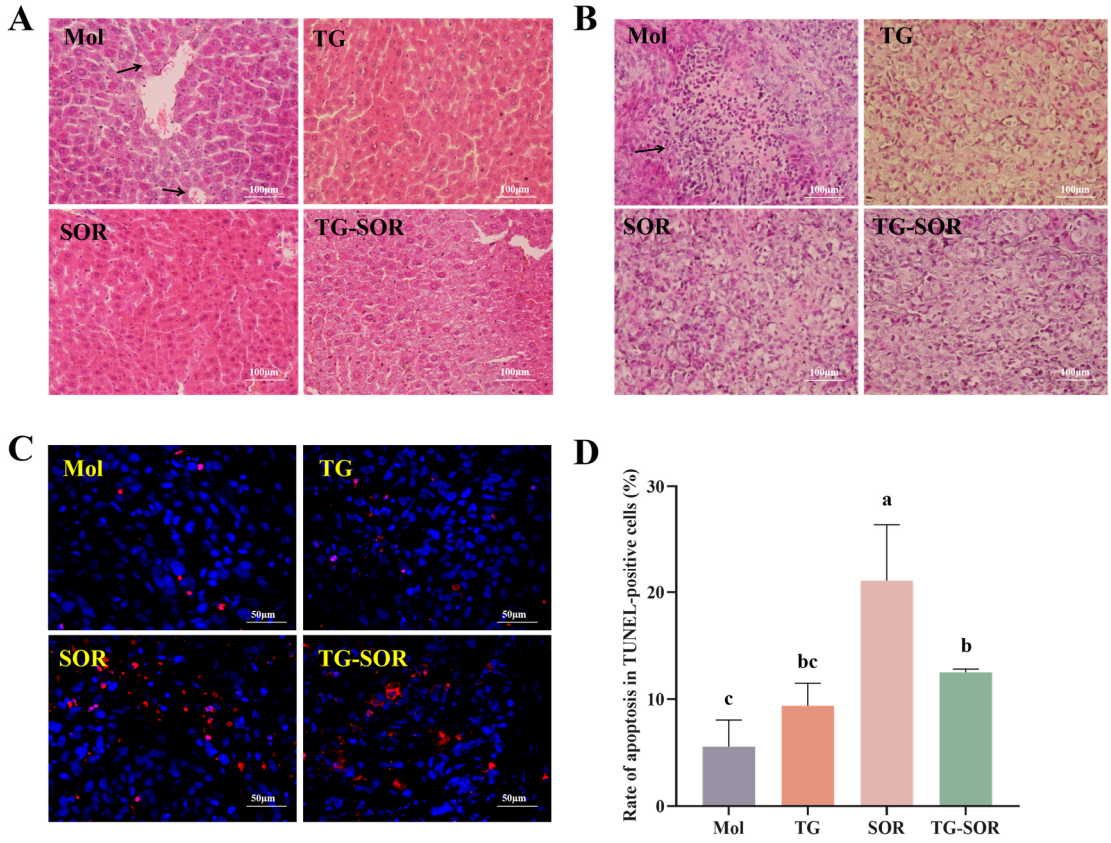

Figure 2 Effect of TG on the tissues of mice with hepatocellular carcinoma. HE staining of liver (A) and tumor (B) tissue slices photographed under an optical microscope (200x). Photographs (C) and quantification (D) of tumor tissue assayed by TUNEL (400x).

The blue color in Figure 2C indicated the nucleus, the red color is stained apoptotic cells, and the bright bule color represents the stained overlapping portion. By analyzing the TUNEL assay of tumor tissues from mice with hepatocellular carcinoma (Figure 2C&D). Comparing the treated groups with Mol group, it was found that the SOR group had the highest rate of apoptosis in TUNEL-positive cells at 21.06%, and the TG, TG-SOR and Mol groups had 9.38%, 12.50% and 5.55%, respectively. This result found that TG can stain tumor cells positively and induce apoptosis, leading to effective alleviation of rapid tumor volume growth. It

was also found that TG cooperated with SOR could increase the apoptosis rate of tumor cells and increase the proportion of late apoptosis.

3.3 Detection of antioxidant indexes in liver tissue

AKP is a membrane-bound enzyme that is found in wide range of organs in the human body, with the highest levels in the liver. Clinical studies have shown that AKP increased when the hepatic system was stimulated by malignant tumor cells [34]. From Figure 3, it could be seen that compared with AKP in the Mol group (Figure 3A), there was a decrease in all treatment groups, with significant differences in both the SOR and TG-SOR groups ($P < 0.05$). GOT, a criterion for the degree of hepatocyte necrosis, is found mainly in the mitochondria of hepatocytes. So, the GOT content in the liver tissue of mice was determined, and the comparison revealed that it was lower in the TG-SOR group than in the Mol group (Figure 3B). GPT is an enzyme involved in protein metabolism in the body and is the most sensitive and specific indicator of hepatocellular injury. Compared with the Mol group, it was found that the GPT content of liver tissue gradually increased in each treatment group (Figure 3C), with the SOR group being the highest and the TG group next to it, and no significant difference existed between each treatment group and the Mol group ($P > 0.05$). Thus, we hypothesized that the liver in the Mol group had very serious lesions, and the treatment group had lower lesions, which suggested that we can use *Cistanche* as an adjuvant treatment for hepatocellular carcinoma patients to protect the liver organ from damage and lesions.

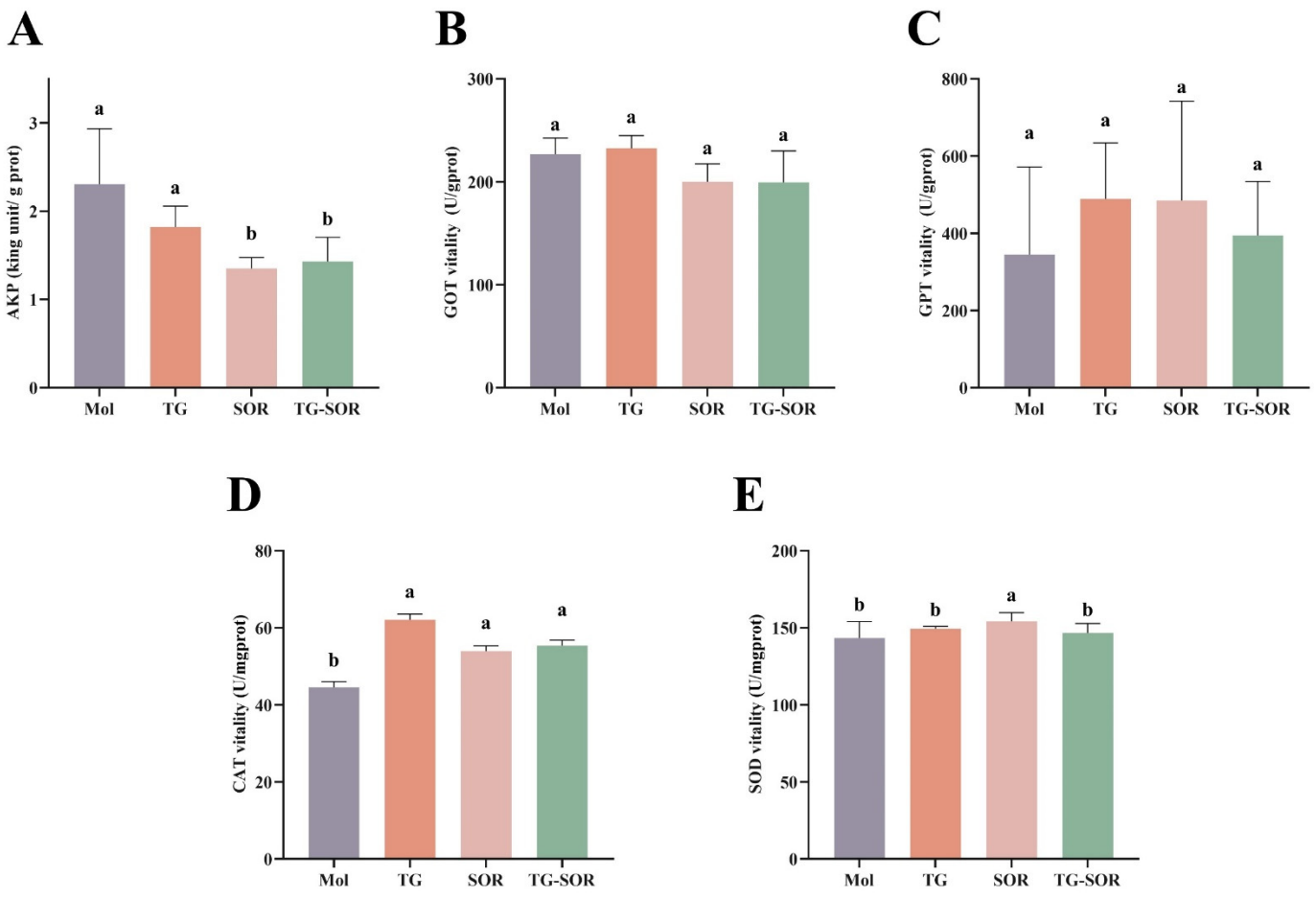

Figure 3 Antioxidant indexes in liver tissue of mice with hepatocellular carcinoma

CAT, the hallmark enzyme of the peroxisome, induces the breakdown of hydrogen peroxide into water and oxygen molecules to protect cells, tissues and organs from the toxic effects of H_2O_2. As compared with the Mol group (Figure 3D), the CAT values of liver tissues increased in all treatment groups, with the TG group showing the greatest increase, followed by the TG-SOR group, and there was a highly significant difference ($P < 0.01$). SOD is an important antioxidant enzyme in living organisms that enables superoxide in the body to be converted into peroxide and oxygen through reactions, and the resulting peroxide is then scavenged by the appropriate catabolic enzymes. It was clear from the trial that the SOD values were slightly higher in the treated group compared to the Mol group (Figure 3E), where there was a significant difference between the SOR and Mol groups ($P < 0.05$). By detecting two antioxidant enzymes, including CAT and SOD, in liver tissues, we found that TG could increase the antioxidant capacity, alleviate the degree of oxidative damage, and improve the antioxidant function of the liver in mice.

3.4 Immunohistochemical changes of GSK-3β, Dsh and β-catenin

The basic theory of immunohistochemistry is to detect proteins in tissue cells according to the antigen-antibody specific binding reaction, and to analyze the degree of chromogenicity for localization, qualitative and relative quantitative studies by color development of the chromogen that labels the antibody. After immunohistochemical staining, the brown color represents the antibody coloring, and the blue color represents the cell nucleus [35]. The browner color, the higher the positivity rate, indicating the more obvious expression of the antibody. By comparing the coloration of the cell membrane, nucleus and cytoplasm, relative quantification, the level of protein expression, can be achieved [35]. As can be seen from Figure 4, the expression of cell proliferation protein Ki67 showed a decreasing trend, confirming that TG could inhibit tumor cell proliferation and induce apoptosis and necrosis of tumor cells. β-catenin and Dsh were significantly decreased in the treated group compared with the Mol group, and the expression was the least in the TG-SOR group (Figure 4B). On the contrary, GSK-3β showed a rising trend, and the TG-SOR group was the most obvious (Figure 4B). Wnt/β-catenin signaling pathway has always attracted much attention[36], it was reported that β-catenin activation could be observed in 20-35% of HCC cases[37]. Studies had found that echinacoside could play an anti-tumor role by inhibiting β-catenin signaling pathway[38, 39]. However, there are few reports on whether the TG of *Cistanche Deserticola* play an anti-hepatocellular carcinoma role by regulating GSK-3β/β-catenin signaling pathway. Additionally, we previously demonstrated *in vitro* that the anticancer effect of TG on HepG2 cells may be achieved by regulating the expression of β-catenin, Dsh and GSK-3β proteins through the Wnt/β-catenin signaling pathway [25]. Tumor tissue immunohistochemistry better reflected the specific expression of these proteins in the cells, which could clearly reflect the characteristics of the accumulation of Wnt/β-catenin from the cytoplasm to the nuclear translocation. It had been reported that β-catenin was mainly in the cytoplasm and nucleus in HepG2 cells, with little expression in the cell membrane. β-catenin in the nucleus could activate the corresponding target genes (c-myc, cylinD1, etc.) to promote cell proliferation, inhibit apoptosis, and promote cell oncology [40]. Therefore, we speculated that TG

achieves hepatocellular carcinoma inhibition by activating GSK-3β to degrade β-catenin, and at the same time served to inhibit tumor migration. This was similar to the results of Shi et al [41] who studied ginsenoside RH2.

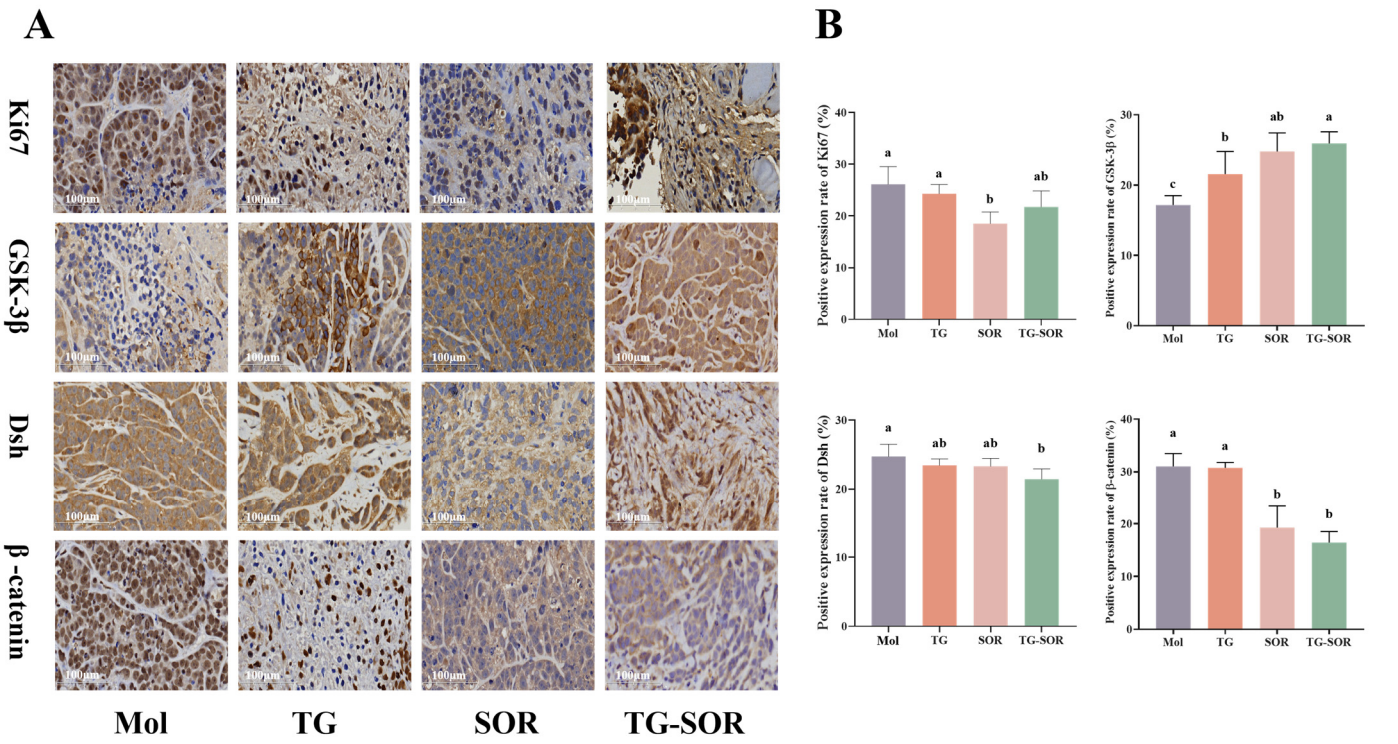

Figure 4 Immunohistochemical detection of protein expression in tumor tissues.

3.5 Serum immune factors in mice with hepatocellular carcinoma

A large amount of clinical data and pilot studies have shown that many cancer patients are immune poorly functioning [42]. First, cellular immunity function becomes poorer, and humoral immunity slowly decreases as the tumor grows. Some studies have reported that *Cistanche* and its active ingredients could alleviate the damage caused by chemotherapeutic drugs on the attack of immune cells and improve the immune function of the body [43].

Table 4 showed that IL-2, IL-10, IL-12p40, IL-17, TNF-α, vascular endothelial growth factor (VEGE), Eotaxin (ETXN), IP-10 and KC were reduced to a certain degree in each treatment group compared with the Mol group, and the TG-SOR group was found to be higher than each group alone. In addition, IFN-γ was a little higher in the TG group than in the Mol group, while it was slightly lower in the SOR group. GM-CSF in mice in the TG-treated group was significantly higher than that in the Mol group, but it was lower in the SOR group.

Table 4 Serum immune factors in mice with hepatocellular carcinoma

Cytokine（pg/ml）	Mol	TG	SOR	TG-SOR
IL-2	4.71 ± 1.92	3.78 ± 1.23	2.99 ± 0.16	3.53 ± 0.81
IL-10	6.06 ± 2.61^{a}	3.17 ± 1.17^{ab}	2.03 ± 1.01^{b}	3.24 ± 2.46^{ab}
IL-12p40	18.24 ± 6.01	13.47 ± 10.25	7.75 ± 5.53	7.94 ± 4.87
IL-17	6.72 ± 2.02	6.61 ± 2.15	3.31 ± 0.67	4.38 ± 1.02
IFN-γ	3.00 ± 0.76	3.03 ± 0.20	2.76 ± 1.03	4.38 ± 2.33
TNF-α	7.99 ± 3.56	7.52 ± 3.25	5.93 ± 3.52	4.03 ± 0.72

VEGE	11.18 ± 14.20	2.42 ± 0.24*	2.50 ± 0.48	2.11 ± 0.19
GM-CSF	1.42 ± 1.72	12.56 ± 14.11	0.20 ± 0.06	13.08 ± 20.90
ETXN	752.33 ± 135.12[a]	649.52 ± 75.25[ab]	476.69 ± 97.9[bc]	413.01 ± 58.50[c]
IP-10	250.54 ± 83.2	154.68 ± 10.20	120.79 ± 87.57	185.08 ± 16.17
KC	137.91 ± 22.61[a]	67.23 ± 20.55[ab]	58.72 ± 61.04[b]	35.12 ± 14.22[b]

Different letters indicate significant differences between groups at the $P < 0.05$ level.

Currently, immunotherapy has recently gained widespread attention as an emerging therapeutic option. Cancer can be promoted by modifying the patient's immune system so that immune cells recognize specific antigens by enhancing immune activity, interfering with immune checkpoint inhibitory signals, preventing infections or inflammatory responses, and synergizing with nonspecific cancer immunotherapy[44]. Immunotherapy can be used in conjunction with current targeted liver cancer drugs to produce combined/synergistic effects[45]. Immune cytokines play a crucial role in the tumor immune microenvironment that determines the fate of tumorigenesis. For example, IL-2 could promote T-lymphocyte activation and stimulate tumor-infiltrating lymphocytes. VEGE could regulate tumor neoangiogenesis and provide conditions for tumor metastasis, and it had been demonstrated that VEGE levels were elevated in patients with liver cancer [46]. TNF-α is mainly secreted by macrophages and promotes hepatocellular carcinogenesis by activating hepatic progenitor cells and inducing cell death in some tumor cell lines [47]. IL-12 is associated with immunotherapy of hepatocellular carcinoma [48], acting as a growth factor for activated T cells and NK cells, stimulating IFN-γ production via resting peripheral blood mononuclear cells (PBMCs), and also playing an important role in tumorigenesis by binding to IL-23α to form IL-23. Studies had demonstrated that IFN-γ inhibited subcutaneous tumors in mice, directly affected tumor growth and metabolism, and induced increased apoptosis of tumor cells [49]. Expression of IL-10 and IL-17 was associated with immune escape from malignant tumors [50-52]. IL-10 activated T-cells, prevented liver damage, is essential in regulating the immune response[53], promoted tumor invasion of other tissues, and IL-10 prevented the secretion of IFN-γ by (natural killer) NK cells, thus reducing the anti-cancer effect of NK cells [54]. GM-CSF is a multifunctional hematopoietic growth factor and an important immune-stimulating factor that induced anti-tumor immune effects in the body [55] [56]. ETXN was used as a predictive maker in cancers such as colon cancer and pancreatic cancer, but it had not been reported in liver cancer [57]. IP-10 had also been reported to be related to cancer metastasis [58]. KC had chemotactic activity on neutrophils and hepatotoxicity [59, 60]. From this, it was clear that TG could improve the body's immune ability, inhibit tumor growth and metabolism, and prevent tumor invasion and transfer to other tissues and other aspects of the anti-tumor effect.

3.6 Untargeted metabolomics of intestinal contents

In recent years, the recognition of malignant tumors such as HCC has gradually changed from a "genetic disease" to a "metabolic disease". Abnormal metabolism of amino acids, lipids and sugars is one of the important features of HCC. Metabolomics reveals the metabolic phenotypic information of biological systems through qualitative and quantitative screening and analysis of all the small-molecule metabolites in biological fluids or tissues, which provides a basis for metabolomics to study the pathogenesis of HCC and explore valuable diagnostic and prognostic markers [61, 62].

The role of metabolites is very important to undertake life activities in cells. A total of 1424 metabolites were identified in this experiment, including 1163 positive ion mode and 726 negative ion mode. In Figure 5A, the highest chemical classification was Lipids and lipid-like molecules 23.596%, followed by organic acids and derivatives 23.455%. The SOR and TG-SOR groups had 122 total metabolic differentiators. Partial least squares discrimination analysis (PLS-DA) is a supervised statistical method for discriminant analysis. The model evaluation parameters (R2Y, Q2) obtained by 7-fold cross-validation. Generally, Q2 > 0.5, indicating that the model is stable and reliable. SOR and TG-SOR groups had R2X=0.287, R2Y=0.988, and Q2=0.661 in the negative ion mode. R2X=0.377, R2Y=0.999, and Q2=0.669 in the positive ion mode. Figure 5B indicated that the PLS-DA model could distinguish between the SOR and TG-SOR groups. Univariate statistical analysis methods are one of the most commonly used statistical analysis methods. Based on the univariate analysis, all the metabolites detected in the positive and negative ion modes (including unidentified metabolites) were analyzed for differences. Figure 5C was suggested that the TG intervention had a significant effect on the metabolic pattern of the mouse organism. Metabolites clustered in the same cluster have similar expression patterns, and may have similar functions or be jointly involved in the same metabolic process or cellular pathway. The results of hierarchical clustering analysis of TG and TG-SOR group metabolomes, significantly different metabolites (VIP > 1, $P < 0.05$) were shown in Figure 5D, indicating that TG could significantly regulate the intestinal metabolite levels of mice. KEGG pathway enrichment analysis is performed on the KEGG pathway in the context of the metabolic pathways in which the species or more closely related species are involved. Figure 5E showed the differential signaling pathways found in metabonomics analysis between SOR and TG-SOR groups, including Retrograde endocannabinoid signaling, butanoate metabolism, morphine addiction, GABAergic synapse, Ferroptosis and other signaling pathways. TG may enhance the role of SOR in inhibiting the occurrence of hepatocellular carcinoma in mice by affecting these key signaling pathways.

In this study, Octanoic acid, Muscone, Phenylbutazone and Glutaric acid were higher in the TG-SOR group. Muscone was found to have anti-hepatocellular carcinoma potential, promoting apoptosis in hepatic cancer cells through endoplasmic reticulum stress and regulating the AMPK/mTOR complex 1 signaling pathway to induce autophagy [63]. It had also been found that FA metabolism could distinguish between patients with virus-induced cirrhosis and hepatocellular carcinoma, which was helpful for early diagnosis, and that TG could increase Octanoic acid levels, which improved the prediction of liver cancer [64]. Lipid metabolism was an important target for the treatment of hepatocellular carcinoma and played a role in HCC progression [65]. Besides, the content of Diisodecyl phthalate, Physcion, Gly-his-lys, Ostruthin, α-tocopherol, Oxalate, Hydroquinidine, Acamprosate were higher in SOR group. Physcion, Gly-his-lys, and Hydroquinidine have been reported to exhibit anti-tumor effects [66][67][68][69]. Also Ostruthin, Gly-his-lys and α-tocopherol had anti-inflammatory effects [68, 70, 71]. Scholars had found an increased number of hepatocellular adenomas in Diisodecyl phthalate-intervened male rasH2 mice in tumor lesions [72]. Therefore, we speculated that TG could assist SOR to reduce the number of hepatocellular adenomas. As a result, TG

significantly modulated the levels of intestinal metabolites in mice and assisted SOR in inhibiting hepatocellular carcinoma development.

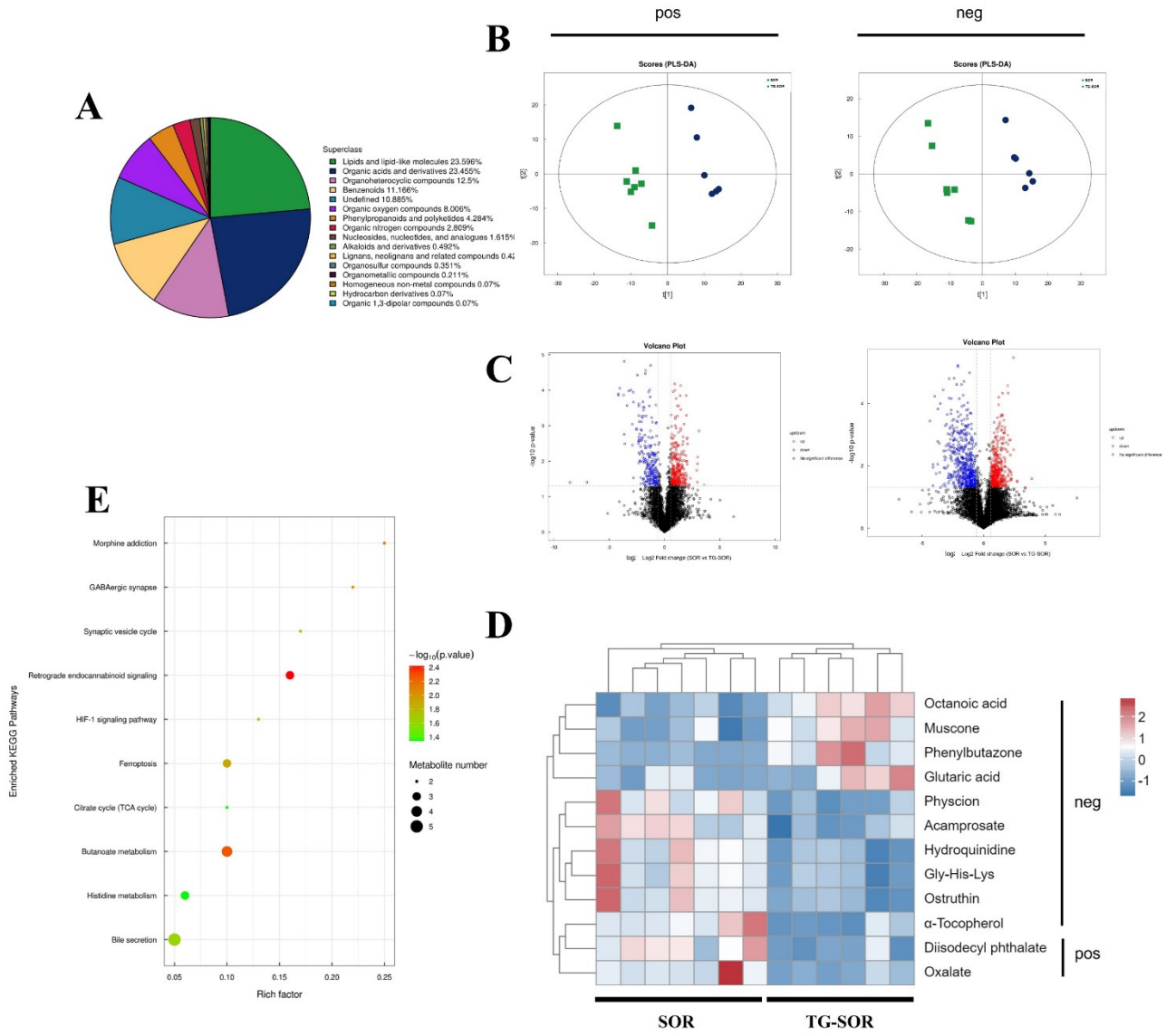

Figure 5 Metabolomics results on intestinal contents in mice with hepatocellular carcinoma. (A) The proportion of identified metabolites in each chemical classification. Different color blocks indicated different chemical classification attribution items and the percentage represents the number of metabolites in the chemical classification attribution item as a percentage of the number of all identified metabolites. (B) The PLS-DA scores in positive and negative ion modes. t [1] represents principal component 1, t [2] represents principal component 2, and ellipses represent 95% confidence intervals. The dots of the same color indicate the individual biological replicates within the group, and the distribution status of the dots reflects the degree of inter- and intra-group variability. (C) Volcano plot in positive and negative ion modes, the horizontal coordinate is the log2 value of the multiplicity of differential expression (Fold Change), and the vertical coordinate is the log10 value of the -log10 of the significance p value. Metabolites satisfying FC > 1.5 and *P* value < 0.05 are shown in red for significantly different metabolites, and metabolites satisfying FC < 0.67 and *P* value < 0.05 are shown in blue. Non-significantly different metabolites are shown in black. (D) The hierarchical clustering thermogram of significant difference metabolites. Each row represents a differential metabolite, each column represents a group of samples, red represents significance up-regulation, blue represents significance down-regulation, and the color shades indicate the degree of up- and down-regulation, and the metabolites with close expression patterns are clustered under the same cluster on the left. (E) KEGG Enrichment Bubble analysis. Each bubble represents a metabolic pathway, the horizontal coordinates of the bubble and the size of the bubble indicate the size of the influence factor of the pathway in the topological analysis, the larger the size, the larger the influence factor. The vertical coordinate where the bubble is located and the color of the bubble indicate the p-value of enrichment analysis (negative common logarithm, i.e., -log10 p-value), the darker the color, the smaller the p-value, and the more significant the degree of enrichment. Rich factor represents the number of differential metabolites in the pathway as a percentage of the number of metabolites annotated in the pathway.

3.7 Sequencing of intestinal contents

The gut microbial composition is significantly changed in patients with HCC [73, 74]. Some scholars had found that specific microbiota may serve as indicators for screening, diagnosis and prognostic characterization of changes in intestinal flora in elderly HCC patients, and may even be considered as a clinical therapeutic target [74].

For Figure 6A, different colors represent different species, corresponding to the legend on the right, the horizontal axis represents different subgroups, and the vertical axis represents the relative abundance of different species. The results revealed that the relative abundance of *Alistipes*, *Roseburia*, *Bacteroides* and *Bifidobacterium spp*. was higher in the TG-SOR group than in the SOR group, while the contrary was observed for *Ruminiclostridium 5* and *Alloprevotella*. *Cistanche* intervention can increase some beneficial bacteria, such as *Bifidobacterium*, *Bacteroides* and *Roseburia* [33, 75]. Principal Co-ordinates Analysis (PCoA), similar to principal components analysis (PCA) analysis, is used to investigate similarities or differences in the composition of sample communities. PCoA is analyzed based on Weighted Unifrac and Unweighted UnifracBeta distances. Horizontal coordinates indicate the first principal component, vertical coordinates indicate the second principal component, and percentages indicate the value of the contribution to sample variation. Figure 6B showed that PcoA could distinguish between these two groups. Taxa heatmap-cluster sample can reflect data information in a two-dimensional matrix or table with a color change, which visually represents the magnitude of the data values in a defined shade of color. Clustering at the species level was performed at the Genus classification level, and the clustered data were represented on a heatmap plot (Figure 6C), which facilitated the visualization of finding out those species that were more or less clustered in which samples or groups. The horizontal axis represents different samples, the vertical axis represents different species, and the shade of the color is related to the abundance of the species, with the darker the color, the higher the relative abundance. The red and green areas in the bar chart of Linear discriminant analysis (LDA) score distribution (Figure 6D) indicated different category, and the red nodes in the dendrites indicated microbial taxa that play an important role in the red category, and the green indicate in the green category. Only species with an LDA score greater than 2 were shown in Figure 6D, the length of the bar graph represented the magnitude of the LDA value. *Enterorhabdus* and *Ruminococcaceae_UCG_013* in genus level are higher than SOR group in TG-SOR, and vice versa for *Intestinimonas*.

The microbiota plays an important role in carcinogenesis, mainly by affecting host cell proliferation and death, altering immune system activity, and influencing host metabolism [76]. For example, TG could increase the relative abundance of *Ruminococcaceae*. A study had found that *Ruminococcaceae* were associated with a reduced risk of HCC, with potential importance for the prevention and control of hepatocellular carcinoma [77]. In another study, it was found that *Ruminococcaceae* gradually decreased in the intestine with the progression of liver cancer, so we speculated that TG slowed down the development of liver cancer [78].

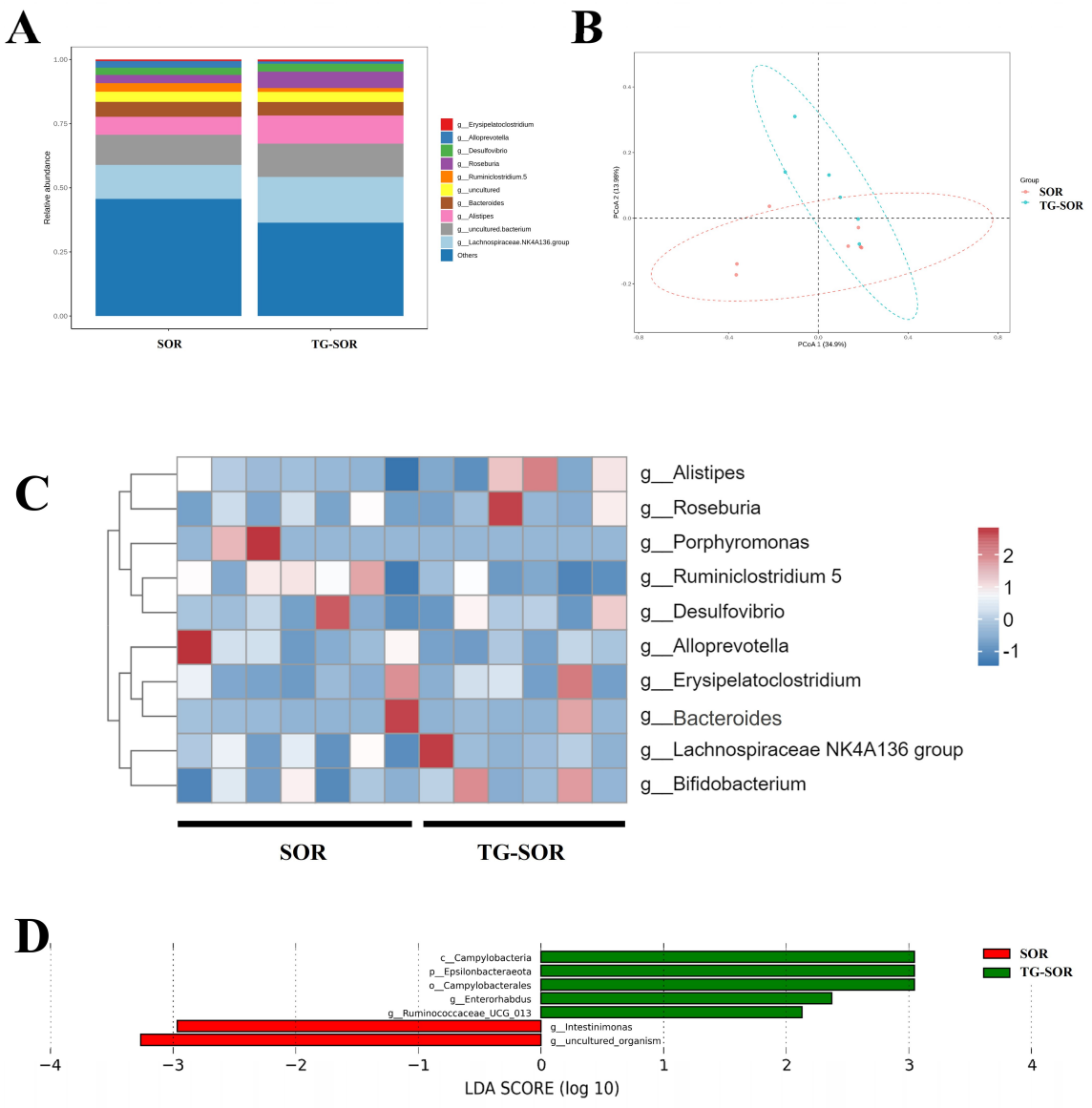

Figure 6 16S rDNA detection results on intestinal contents in mice. (A) The bar chart of species composition abundance at the genus level. (B) Principal Co-ordinates Analysis. (C) Taxa heatmap-cluster sample. (D) The distribution bar chart of linear discriminant analysis (LDA) values.

4. Conclusions

The schematic overview of mechanism underlying TG enhancing the inhibitory effect of SOR on hepatocellular carcinoma in mice can be seen from Figure 7. This experiment revealed the potential value of *Cistanche deserticola* combined with Sorafenib in the therapy of hepatocellular carcinoma, signifying that the coordinated utilization of this natural health functional food and medicine had the development prospect for preventive and adjunctive treatment of liver cancer. However, the number of animals in this experimental model was small, which may lead to the inaccuracy of the results caused by animal stress reaction. Therefore, the synergistic effect of *Cistanche deserticola* and Sorafenib will be further considered when the number of mice is expanded in the future and the specific components in the TG of *Cistanche deserticola* will be deeply excavated to study its anti-hepatocellular carcinoma effect. In addition, based on the current research results, it

is planned to conduct further experiments to verify its mechanism of action and ensure the scientific and reliable research conclusions.

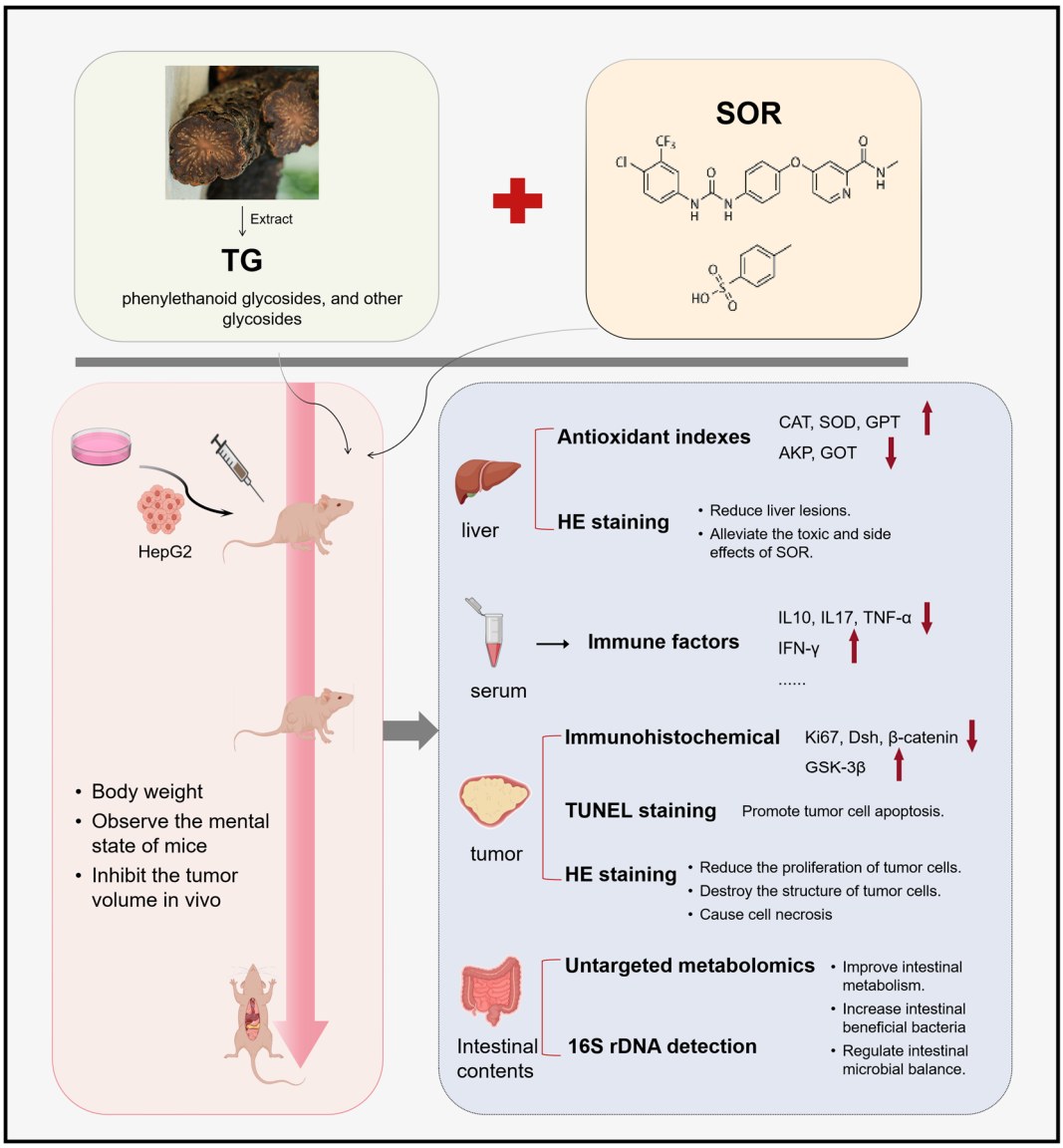

Figure 7 Schematic overview of mechanism underlying TG enhancing the inhibitory effect of SOR on hepatocellular carcinoma in mice.

Acknowledgments

This work was supported by the National Key Research and Development Program of China (2023YFF1103800).

Declaration of interest statement

The authors declare no conflicts of interest.

Ethics statement

The animal experimental protocol was authorized by the Animal Care and Use Ethics Committee of Beijing Union University (Approval No: 20200914), and all experiments were conducted in accordance with the Guide for the Care and Use of Laboratory Animals.

References

[1] Ma G., Chen J., Wei T., Wang J., Chen W. Inhibiting roles of foxa2 in liver cancer cell migration and invasion by transcriptionally suppressing microrna-103a-3p and activating the grem2/lats2/yap axis [J]. *Cytotechnology*, 2021, 73(4): 523-537.

[2] Bray F., Laversanne M., Sung H., Ferlay J., Siegel R.L., Soerjomataram I., Jemal A. Global cancer statistics 2022: Globocan estimates of incidence and mortality worldwide for 36 cancers in 185 countries [J]. *CA: A Cancer Journal for Clinicians*, 2024, 74(3): 229-263.

[3] Sung H., Ferlay J., Siegel R.L., Laversanne M., Soerjomataram I., Jemal A., Bray F. Global cancer statistics 2020: Globocan estimates of incidence and mortality worldwide for 36 cancers in 185 countries [J]. *CA: A Cancer Journal for Clinicians*, 2021, 71(3): 209-249.

[4] Gera S., Ettel M., Acosta-Gonzalez G., Xu R. Clinical features, histology, and histogenesis of combined hepatocellular-cholangiocarcinoma [J]. *World Journal of Hepatology*, 2017, 9(6).

[5] Xu W.-h. The anti-tumor effect of parthenolide by inducing apoptosis and autophagy of human hepatoma cells and its mechanism [D]. Tsingtao; Qingdao university, 2020.

[6] Hou X.-t., Su D.-q., Qi X.-x., Liiu T. Effect of phenylethanol glycosides from cistanche deserticola on autophagy of tumor cells in h22 tumor-bearing mice [J]. *Journal of Toxicology*, 2022, 36(02): 137-141.

[7] Hu Q., You S.-p., Liu T., Wang B., Liu X., Jiang Y.-d. An investigation on the anti-liver cancer effect of cistanche [J]. *Carcinogenesis,Teratogenesis & Mutagenesis*, 2018, 30(03): 194-199.

[8] Qi X.-x., You S.-p., He Z.-x., Zhao J., Liu T. Effect of cistanche deserticola phenylethanol glycoside on proliferation and apoptosis of hepg2 cells in viro [J]. *Journal of Xinjiang Medical University*, 2021, 44(09): 1041-1047.

[9] G. S.Z., W. X.H., B. J.F., P L. Sorafenib plus capecitabine for patients with advanced hepatocellular caicinoma [J]. *China Pharmacy*, 2008, (11): 848-849.

[10] Tang W., Chen Z., Zhang W., Cheng Y., Zhang B., Wu F., Wang Q., Wang S., Rong D., Reiter F.P., De Toni E.N., Wang X. The mechanisms of sorafenib resistance in hepatocellular carcinoma: Theoretical basis and therapeutic aspects [J]. *Signal Transduct Target Ther*, 2020, 5(1): 87.

[11] Sun Y., Song Y.-y., Zhang C., Lu Y.-z., Zheng G.-h., Tian X.-x., Qiu Z.-p., Chen L. Effect and mechanism of celastrol on the proliferation of hepatocellular carcinoma hepg2 cells by activatingg ampk signal pathway [J]. *China Pharmacist*, 2021, 24(11): 1961-1966+1982.

[12] Villarruel-Melquiades F., Hernandez-Gallegos E., Solano-Agama C., Mendoza-Garrido M.E., Camacho J. The combination sorafenib-raloxifene-loratadine as a novel potential therapeutic approach against human liver cancer [J]. *In Vivo*, 2023, 37(3): 1156-1163.

[13] Huang Y., Wang K., Gu C., Yu G., Zhao D., Mai W., Zhong Y., Liu S., Nie Y., Yang H. Berberine, a natural plant alkaloid, synergistically sensitizes human liver cancer cells to sorafenib [J]. *Oncology Reports*, 2018.

[14] Abdu S., Juaid N., Amin A., Moulay M., Miled N. Effects of sorafenib and quercetin alone or in combination in treating hepatocellular carcinoma: In vitro and in vivo approaches [J]. *Molecules*, 2022, 27(22).

[15] De Vos W.M., Tilg H., Van Hul M., Cani P.D. Gut microbiome and health: Mechanistic insights [J]. *Gut*, 2022, 71(5): 1020-1032.

[16] Mima K., Baba H. The gut microbiome, antitumor immunity, and liver cancer [J]. *Hepatobiliary surgery and nutrition*, 2019, 8(1): 67-68.

[17] Tripathi A., Debelius J., Brenner D.A., Karin M., Loomba R., Schnabl B., Knight R. The gut-liver axis and the intersection with the microbiome [J]. *Nature reviews Gastroenterology & hepatology*, 2018, 15(7): 397-411.

[18] Roderburg C., Luedde T. The role of the gut microbiome in the development and progression of liver cirrhosis and hepatocellular carcinoma [J]. *Gut microbes*, 2014, 5(4): 441-445.

[19] Shen S., Khatiwada S., Behary J., Kim R., Zekry A. Modulation of the gut microbiome to improve clinical outcomes in hepatocellular carcinoma [J]. *Cancers*, 2022, 14(9).

[20] Behary J., Amorim N., Jiang X.T., Raposo A., Gong L., Mcgovern E., Ibrahim R., Chu F., Stephens C., Jebeili H., Fragomeli V., Koay Y.C., Jackson M., O'sullivan J., Weltman M., Mccaughan G., El-Omar E., Zekry A. Gut microbiota impact on the peripheral immune response in non-alcoholic fatty liver disease related hepatocellular carcinoma [J]. *Nature communications*, 2021, 12(1): 187.

[21] Ponziani F.R., Bhoori S., Castelli C., Putignani L., Rivoltini L., Del Chierico F., Sanguinetti M., Morelli D., Paroni Sterbini F., Petito V., Reddel S., Calvani R., Camisaschi C., Picca A., Tuccitto A., Gasbarrini A., Pompili M., Mazzaferro V. Hepatocellular carcinoma is associated with gut microbiota profile and inflammation in nonalcoholic fatty liver disease [J]. *Hepatology (Baltimore, Md)*, 2019, 69(1): 107-120.

[22] Yu L.X., Schwabe R.F. The gut microbiome and liver cancer: Mechanisms and clinical translation [J]. *Nature reviews Gastroenterology & hepatology*, 2017, 14(9): 527-539.

[23] Dapito D.H., Mencin A., Gwak G.Y., Pradere J.P., Jang M.K., Mederacke I., Caviglia J.M., Khiabanian H., Adeyemi A., Bataller R., Lefkowitch J.H., Bower M., Friedman R., Sartor R.B., Rabadan R., Schwabe R.F. Promotion of hepatocellular carcinoma by the intestinal microbiota and tlr4 [J]. *Cancer cell*, 2012, 21(4): 504-516.

[24] Yoshimoto S., Loo T.M., Atarashi K., Kanda H., Sato S., Oyadomari S., Iwakura Y., Oshima K., Morita H., Hattori M., Honda K., Ishikawa Y., Hara E., Ohtani N. Obesity-induced gut microbial metabolite promotes liver cancer through senescence secretome [J]. *Nature*, 2013, 499(7456): 97-101.

[25] Feng D., Wang J., Jiang Y.-j., Zhou S.-q., Duan H., Guo Y., Zhao J., Yan W.-j. Effects of total glycosides of *cistanche deserticola* on proliferation, apoptosis and expression of wnt/β-catenin signaling pathway related protein of hepg2 cells [J]. *Science and Technology of Food Industry*, 2023, 44(20): 389-397.

[26] Feng D., Chang X., Jiang Y.-j., Guo Y., Zhao J., Zhao J.-y., Sun Q.-d., Song W., Cui Q.-q., Yan W.-j. Optimization of aqueous extraction preparation technology of *cistanche deserticola* by response surface methodology and its activity research [J]. *Science and Technology of Food Industry*, 2023, 44(05): 139-148.

[27] Feng D., Wang J., Jiang Y.-j., Zhou S.-q., Duan H., Li J.-y., Yan W.-j. Effect of total glycosides of cistanche deserticola on hepg2 liver cancer mice [J]. *Food Science*, 2024, 45(6): 120-129.

[28] Liu L., Cao Y., Chen C., Zhang X., Mcnabola A., Wilkie D., Wilhelm S., Lynch M., Carter C. Sorafenib blocks the raf/mek/erk pathway, inhibits tumor angiogenesis, and induces tumor cell apoptosis in hepatocellular carcinoma model plc/prf/5 [J]. *Cancer Research*, 2006, 66(24): 11851-11858.

[29] Wang Z., Zhao Z., Wu T., Song L., Zhang Y. Sorafenib-irinotecan sequential therapy augmented the anti-tumor efficacy of monotherapy in hepatocellular carcinoma cells hepg2 [J]. *Neoplasma*, 2015, 62(02): 172-179.

[30] Sun Y., Xiao F., Sun H., Zhang L., Chen W., Du L., Sun C., Zhang W., Xu Q., Miao C., Wang L. Transcriptome analysis of tumor-derived mesenchymal progenitor cells shows that chst15 is a fibrosis regulator of retroperitoneal liposarcoma [J]. *Ann Transl Med*, 2022, 10(6): 360.

[31] Huang H., Liu Z., Qi X., Gao N., Chang J., Yang M., Na S., Liu Y., Song R., Li L., Chen G., Zhou H. Rhubarb granule promotes diethylnitrosamine-induced liver tumorigenesis by activating the oxidative branch of pentose phosphate pathway via g6pd in rats [J]. *J Ethnopharmacol*, 2021, 281: 114479.

[32] Feng D., Zhou S.Q., Zhou Y.X., Jiang Y.J., Sun Q.D., Song W., Cui Q.Q., Yan W.J., Wang J. Effect of total glycosides of cistanche deserticola on the energy metabolism of human hepg2 cells [J]. *Front Nutr*, 2023, 10: 1117364.

[33] Samanta S. Potential impacts of prebiotics and probiotics on cancer prevention [J]. *Anti-Cancer Agents in Medicinal Chemistry*, 2022, 22(4): 605-628.

[34] Song S.-t., Zhu F., Sun Y., Ye J., Liu F. Diagnostic value of combined detection of serum afp, afu and alp in primary liver cancer [J]. *International Journal of Digestive Diseases*, 2017, 37(03): 177-179.

[35] Tang C.-l., Kuang Z.-p., Yang F. The dynamic changes of β-catenin in the process of mice liver cancer formation chemically [J]. *Journal of Modern Oncology*, 2013, 21(06): 1204-1208.

[36] Clevers H., Nusse R. Wnt/beta-catenin signaling and disease [J]. *Cell*, 2012, 149(6): 1192-1205.

[37] Russell J.O., Monga S.P. Wnt/beta-catenin signaling in liver development, homeostasis, and pathobiology [J]. *Annual review of pathology*, 2018, 13: 351-378.

[38] Cheng-Huai T. Echinacoside inhibits breast cancer cells by suppressing wnt/β-catenin signaling pathway [D]. Chongqing; Chongqing Medical University, 2020.

[39] Lei F., Qiu-Limh M., Lin S., Yi W. Echinacein inhibits the proliferation of acute myeloid leukemia cells by suppressing sox4/wnt/beta-catenin signal [J]. *Immunological Journal*, 2020, 36(02): 138-142.

[40] Shen H.-j., Chen G.-y., Zhan J.-x., Hu B., Jin S.-l. Expression of β-catenin and its significance in the l2、wb、hepg2、smcc cells [J]. *Chinese Journal of Practical Surgery*, 2011, 31(S2): 46-47.

[41] Shi Q.-q., Zuo G.-w., Feng Z.-q., Zhao L.-c., Li J., Chen D.-l. Study on anti-hepatoma effect of ginsenoside rh2 and mechanism of degradation of β-catenin through activating gsk-3β [J]. *Chinese Traditional and Herbal Drugs*, 2016, 47(18): 3231-3238.

[42] Zhao C., Lin G., Wu D., Liu D., You L., Högger P., Simal-Gandara J., Wang M., Da Costa J.G.M., Marunaka Y., Daglia M., Khan H., Filosa R., Wang S., Xiao J. The algal polysaccharide ulvan suppresses growth of hepatoma cells [J]. *Food Frontiers*, 2020, 1(1): 83-101.

[43] Liu Z.-q., Chen Q.-t., Li Y., Song Y., Sun H.-l. Influences of roucongrong(herba cistanchis) on hematopoietic function and immune function in tumor-bearing mice after chemotherapy [J]. *Journal of Beijing University of Traditional Chinese Medicine*, 2010, 33(11): 758-761.

[44] Anwanwan D., Singh S.K., Singh S., Saikam V., Singh R. Challenges in liver cancer and possible treatment approaches [J]. *Biochim Biophys Acta Rev Cancer*, 2020, 1873(1): 188314.

[45] Zhao X., Chen Q., Liu W., Li Y., Tang H., Liu X., Yang X. Codelivery of doxorubicin and curcumin with lipid nanoparticles results in improved efficacy of chemotherapy in liver cancer [J]. *Int J Nanomedicine*, 2015, 10: 257-270.

[46] Song C.-r., Nan R., Liu Y.-g., Li J.-t., Yan S.-g., Wei H.-l., Xi Q., Kou X.-n. Effect of yipi yanggang decoction on bfgf、vegf、afp-l3 and immune function in patients undergoing tace surgery for primary liver cancer [J]. *Journal of Liaoning University of Traditional Chinese Medicine*, 2022, 24(01): 80-84.

[47] Jing Y., Sun K., Liu W., Sheng D., Zhao S., Gao L., Wei L. Tumor necrosis factor-α promotes hepatocellular carcinogenesis through the activation of hepatic progenitor cells [J]. *Cancer Letters*, 2018, 434: 22-32.

[48] Bonnans C., Thomas G., He W., Jung B., Chen W., Liao M., Heyen J., Buetow B., Pillai S., Matsumoto D., Chaparro-Riggers J., Salek-Ardakani S., Qu Y. Cd40 agonist-induced il-12p40 potentiates hepatotoxicity [J]. *J Immunother Cancer*, 2020, 8(1).

[49] Karin M., Greten F.R. Nf-kappab: Linking inflammation and immunity to cancer development and progression [J]. *Nat Rev Immunol*, 2005, 5(10): 749-759.

[50] He Y.-y., Luo B.-t., Lu Y.-z. Research progress on the role of immunosuppressive cells and cytokines in anti-tumor immune response in tumor microenvironment [J]. *Shandong Medical Journal*, 2019, 59(06): 88-92.

[51] Kurte M., Lopez M., Aguirre A., Escobar A., Aguillon J.C., Charo J., Larsen C.G., Kiessling R., Salazar-Onfray F. A synthetic peptide homologous to functional domain of human il-10 down-regulates expression of mhc class i and transporter associated with antigen processing 1/2 in human melanoma cells [J]. *J Immunol*, 2004, 173(3): 1731-1737.

[52] Molina M.F., Abdelnabi M.N., Fabre T., Shoukry N.H. Type 3 cytokines in liver fibrosis and liver cancer [J]. *Cytokine*, 2019, 124: 154497.

[53] Ali A.K., Komal A.K., Almutairi S.M., Lee S.H. Natural killer cell-derived il-10 prevents liver damage during sustained murine cytomegalovirus infection [J]. *Front Immunol*, 2019, 10: 1-14.

[54] Liu L.-l., Kang Z.-l., Chu Y.-k. Cytokines and tumor immunity [J]. *Shanxi Medical Journal*, 2013, 42(11): 1250-1252.

[55] Nemunaitis J., Barve M., Orr D., Kuhn J., Magee M., Lamont J., Bedell C., Wallraven G., Pappen B.O., Roth A., Horvath S., Nemunaitis D., Kumar P., Maples P.B., Senzer N. Summary of bi-shrnafurin/gm-csf augmented autologous tumor cell immunotherapy (fang™) in advanced cancer of the liver [J]. *Oncology*, 2014, 87(1): 21-29.

[56] Zhou Y., Yang L. Role and clinical application of granulocyte-macrophage colony-stimulating factor in tumor immunotherapy [J]. *Journal of Diagnostics Concepts & Practice*, 2021, 20(04): 407-413.

[57] Zajkowska M., Mroczko B. From allergy to cancer—clinical usefulness of eotaxins [J]. *Cancers*, 2021, 13(1).

[58] Clark A.M., Heusey H.L., Griffith L.G., Lauffenburger D.A., Wells A. Ip-10 (cxcl10) can trigger emergence of dormant breast cancer cells in a metastatic liver microenvironment [J]. *Frontiers in Oncology*, 2021, 11.

[59] Rovai L., Herschman H. The murine neutrophil-chemoattractant chemokines lix, kc, and mip-2 have distinct induction kinetics, tissue distributions, and tissue-specific sensitivities to glucocorticoid regulation in endotoxemia [J]. *JOURNAL OF LEUKOCYTE BIOLOGY*, Smith, JB 54(4): 494-502.

[60] Stefanovic L., Brenner D., Stefanovic B. Direct hepatotoxic effect of kc chemokine in the liver without infiltration of neutrophils [J]. *EXPERIMENTAL BIOLOGY AND MEDICINE*, 2005, 230(8): 573-586.

[61] Lyu Q., Deng H., Wang S., El-Seedi H., Cao H., Chen L., Teng H. Dietary supplementation with casein/cyanidin-3-o-glucoside nanoparticles alters the gut microbiota in high-fat fed c57bl/6 mice [J]. *Food Chemistry*, 2023, 412.

[62] Lyu Q., Chen L., Lin S., Cao H., Teng H. A designed self-microemulsion delivery system for dihydromyricetin and its dietary intervention effect on high-fat-diet fed mice [J]. *Food Chemistry*, 2022, 390.

[63] Qi W., Li Z., Yang C., Jiangshan Dai J., Zhang Q., Wang D., Wu C., Xia L., Xu S. Inhibitory mechanism of muscone in liver cancer involves the induction of apoptosis and autophagy [J]. *Oncology Reports*, 2020.

[64] Nomair A., Madkour M., Shamseya M., Elsheredy H., Shokr A. Profiling of plasma metabolomics in patients with hepatitis c-related liver cirrhosis and hepatocellular carcinoma [J]. *Clinical and Experimental Hepatology*, 2019, 5(4): 317-326.

[65] Pope E.D., Kimbrough E.O., Vemireddy L.P., Surapaneni P.K., Copland J.A., Mody K. Aberrant lipid metabolism as a therapeutic target in liver cancer [J]. *Expert Opinion on Therapeutic Targets*, 2019, 23(6): 473-483.

[66] Jiang H., Tang W., Song Y., Jin W., Du Q. Induction of apoptosis by metabolites of rhei radix et rhizoma (da huang): A review of the potential mechanism in hepatocellular carcinoma [J]. *Frontiers in Pharmacology*, 2022, 13.

[67] Pan X.-p., Wang C., Li Y., Huang L.-h. Physcion induces apoptosis through triggering endoplasmic reticulum stress in hepatocellular carcinoma [J]. *Biomedicine & Pharmacotherapy*, 2018, 99: 894-903.

[68] Pickart L., Margolina A. Regenerative and protective actions of the ghk-cu peptide in the light of the new gene data [J]. *International Journal of Molecular Sciences*, 2018, 19(7).

[69] Yavuz M., Demircan T. A potent ion channel blocker, hydroquinidine, exhibits strong anti-cancer activity on colon, pancreatic, and hepatocellular cancer cells [J]. *Molecular Biology Reports*, 2023, 50(3): 2611-2621.

[70] Tuan Anh H.L., Kim D.-C., Ko W., Ha T.M., Nhiem N.X., Yen P.H., Tai B.H., Truong L.H., Long V.N., Gioi T., Hong Quang T., Minh C.V., Oh H., Kim Y.-C., Kiem P.V. Anti-inflammatory coumarins from paramignya trimera [J]. *Pharmaceutical Biology*, 2017, 55(1): 1195-1201.

[71] Sharma R., Vinayak M. A-tocopherol attenuates nf-κb activation and pro-inflammatory cytokine il-6 secretion in cancer-bearing mice [J]. *Bioscience reports*, 2011, 31(5): 421-428.

[72] Cho W.-S., Jeong J., Choi M., Park S.N., Han B.S., Son W.-C. 26-week carcinogenicity study of di-isodecyl phthalate by dietary administration to cb6f1-rash2 transgenic mice [J]. *Archives of Toxicology*, 2010, 85(1): 59-66.

[73] Feng J., Wu Y., Dai P., Wang D., Liu L., Chai B. Gut microbial signatures of patients with primary hepatocellular carcinoma and their healthy first-degree relatives [J]. *Journal of Applied Microbiology*, 2023, 134(10).

[74] Zhang W., Xu X., Cai L., Cai X. Dysbiosis of the gut microbiome in elderly patients with hepatocellular carcinoma [J]. *Scientific Reports*, 2023, 13(1).

[75] Zhang C., Ma K., Nie K., Deng M., Luo W., Wu X., Huang Y., Wang X. Assessment of the safety and probiotic properties of roseburia intestinalis: A potential “next generation probiotic” [J]. *Frontiers in Microbiology*, 2022, 13.

[76] Hou K., Wu Z.-X., Chen X.-Y., Wang J.-Q., Zhang D., Xiao C., Zhu D., Koya J.B., Wei L., Li J., Chen Z.-S. Microbiota in health and diseases [J]. *Signal Transduction and Targeted Therapy*, 2022, 7(1).

[77] Ma J., Li J., Jin C., Yang J., Zheng C., Chen K., Xie Y., Yang Y., Bo Z., Wang J., Su Q., Wang J., Chen G., Wang Y. Association of gut microbiome and primary liver cancer: A two-sample mendelian randomization and case–control study [J]. *Liver International*, 2023, 43(1): 221-233.

[78] N. Jiang X.S., Y.-M. PENG, W.-N. WANG, Z. SONG. Association of disease condition with changes in intestinal flora, and plasma endotoxin and vascular endothelial growth factor levels in patients with liver cancer [J]. *European Review for Medical and Pharmacological Sciences*, 2020, 24: 9.